0026-895X/08/7301-224–234$20.00
MOLECULAR PHARMACOLOGY
Copyright © 2008 The American Society for Pharmacology and Experimental Therapeutics
Mol Pharmacol 73:224–234, 2008

Vol. 73, No. 1
38901/3286917
Printed in U.S.A.

The Unusual State-Dependent Affinity of $P2X_3$ Receptors Can Be Explained by an Allosteric Two-Open-State Model

R. Karoly, A. Mike, P. Illes, and Z. Gerevich

Department of Pharmacology, Institute of Experimental Medicine, Hungarian Academy of Sciences, Budapest, Hungary (R.K., A.M.); and Rudolf Boehm Institute of Pharmacology and Toxicology, Leipzig, Germany (P.I., Z.G.)

Received June 11, 2007; accepted October 9, 2007

ABSTRACT

High-affinity desensitization (HAD) by nanomolar agonists was described to shape the ability of $P2X_3$ receptors for mediating pain sensation. These receptors are activated by micromolar ATP, but nanomolar ATP is sufficient to effectively desensitize them. The mechanism behind HAD is still obscure. It has been suggested (*J Neurosci* **25:**7359–7365, 2005) that HAD can happen only if the receptor has previously been activated and desensitized by high agonist concentrations. It was not clear, however, whether the high-affinity site was different from the conventional binding site and which mechanism led to its exposure during desensitization. A subsequent article (*Mol Pharmacol* **70:**373–382, 2006) argued that HAD could also occur without preceding desensitization, because even resting receptors expose high-affinity binding sites. To support this hypothesis, a kinetic model was proposed that could reproduce all major phenomena observed experimentally. We attempted to improve this model and used it to simulate the agonist-induced formation of the high-affinity binding site. We collected electrophysiological data using HEK 293 cells expressing human $P2X_3$ receptors and fitted simulated currents to experimentally acquired currents. A simple allosteric kinetic model in which only triliganded receptors could open failed to reproduce receptor behavior; introduction of an additional diliganded open state was necessary. Simulation with this model gave results that were in good agreement with experimental data. By using simulations and experiments, we analyzed the process of high-affinity binding site formation upon agonist exposure and propose an explanation, which helps to resolve the apparent conflict regarding the mechanism of HAD.

Rapid desensitization (within ~100 ms) and very slow recovery from desensitization (requiring several minutes) are the hallmark of $P2X_3$ [and also of $P2X_1$ (Rettinger and Schmalzing, 2003)] receptors (North, 2002). In the study of this phenomenon, it has been shown that agonists compete for the same binding sites, and the recovery rate will be determined by the type of agonist occupying the binding sites of the receptors at the beginning of washout (Sokolova et al., 2004). Extremely low concentrations of agonists were found to be able to effectively inhibit agonist-evoked currents, presumably by inducing desensitization of the receptors. No detectable currents were evoked at these low concentrations; in fact, a ~80- to 800-fold difference was found between IC_{50} and EC_{50} values of the same agonist.

The ability of low nanomolar agonist concentrations to induce desensitization was questioned by an elegant study of Pratt et al. (2005), where the ability of agonists to prevent recovery from desensitization was compared with their ability to induce desensitization. Intriguingly, and in contrast to previous results, no inhibition by nanomolar agonists was found without previous activation and desensitization.

Dealing with a mechanism in which agonists cannot induce desensitization but, once it is attained, are able to stabilize desensitized conformation, presumes that equilibrium distribution of receptor states will be different, depending on whether receptors were in a resting or a desensitized state at the beginning of low concentration agonist application. This idea is incompatible with conventional models of receptor kinetics; a unique mechanism unlike the ones valid for other desensitizing receptors should have been proposed. However, no detailed hypothesis was offered for the mechanism by which this mysterious "transfiguration" of the binding sites occurred. Thus, it is not clear whether formation of high-affinity binding sites is supposed to involve formation of novel sites or reconstruction of existing ones. It is also unclear why the authors had to suppose "rebinding" as a requirement of HAD (Pratt et al., 2005) (i.e., why staying bound would not suffice).

In a subsequent article (Sokolova et al., 2006), a cleverly

This work was supported by grants from the Deutsche Forschungsgemeinschaft (IL 20/11-3) and the Hungarian Research Fund (T 037659). A.M. is the recipient of a Janos Bolyai Research Fellowship.

Article, publication date, and citation information can be found at http://molpharm.aspetjournals.org.

doi:10.1124/mol.107.038901.

ABBREVIATIONS: HEK, human embryonic kidney; HAD, high-affinity desensitization; meATP, methylene ATP; MWC, Monod-Wyman-Changeux.

designed attempt was made to demystify HAD of $P2X_3$ receptors. To mechanistically explain findings with low concentration agonists, a kinetic model of the $P2X_3$ receptor was proposed. Simulations using this model adequately reproduced experimental data. By experimentation and simulation, the possibility of HAD was demonstrated even in the absence of preceding desensitization. However, the properties of the model used in this study cast doubt on this conclusion. Parameter optimization was probably done using a fitting algorithm, and the assumption of microscopic reversibility was not used as a constraint. The model predicts that uniliganded receptors cannot open but only desensitize, diliganded receptors can neither desensitize nor open, and triliganded receptors can only desensitize via open state.

To be able to test hypotheses, gain more insight into the mechanisms of receptor activation and desensitization, and resolve contradicting results of previous publications, we decided that it was necessary to improve this model. We chose to construct an "allosteric" type of model (Monod et al., 1965) to ensure that it is thermodynamically feasible and as simple as possible (i.e., has few free parameters). In electrophysiological experiments, we obtained kinetic data in a range of different concentrations and used them to test different models. We started this approach with the simplest possible model and increased the complexity only when it was proven necessary. A 10-state model with only eight free parameters reproduced all experimental data reasonably well.

Using electrophysiology and modeling, the following specific questions were addressed: 1) Does increased affinity indeed require preceding agonist exposure? 2) Is the high-affinity site different from the conventional binding site? 3) Do we need to suppose unbinding and rebinding? 4) What is the mechanism of binding site "transfiguration"? 5) Do low concentration agonist-induced desensitization and recovery from desensitization converge to the same equilibrium distribution of receptors? (If they do, the conflicting views are due simply to the methodological problem of not perfusing the agonists long enough.) 6) Can a conventional allosteric model reproduce kinetic behavior of the receptor (in particular, the extreme differences in the affinities of resting and desensitized conformations)?

We were able, based on the simulations, to answer the above questions, and to propose an explanation of binding site "transfiguration," which resolves contradictions between previous experimental findings. We show that if we assume the simplest allosteric mechanism, increased affinity upon preceding agonist binding will unavoidably occur, and it requires no unique mechanism.

Materials and Methods

Culturing of HEK293-$hP2X_3$ Cells. Methods of maintenance of HEK293 cells and their stable transfection with $hP2X_3R$ cDNA have been described previously (Fischer et al., 2003). Cells were kept in Dulbecco's modified Eagle's medium also containing 25 mM HEPES, 110 μg/ml sodium pyruvate, 1 mg/ml D-glucose, 4 μg/ml pyridoxine (Invitrogen, Karlsruhe, Germany), 2 mM L-glutamine, 1% nonessential amino acids (all Sigma, Deisenhofen, Germany), 10% fetal bovine serum, and 50 μg/ml G-418 (Geneticin) (both from Invitrogen) at 37°C and 10% CO_2 in humidified air. They were plated on 35-mm plastic dishes (Sarstedt, Nürnberg, Germany) for electrophysiological recordings.

Whole-Cell Patch-Clamp Recordings. Whole-cell patch-clamp recordings were performed 2 to 6 days after the splitting of permanently transfected HEK293 cells at room temperature (20–22°C), using an Axopatch 200B patch-clamp amplifier (Molecular Devices, Sunnyvale, CA). Patch pipettes (3–5 MΩ) for HEK293 cells were filled with intracellular solution of the following composition: 135 mM CsCl, 2 mM $MgCl_2$, 20 mM HEPES, 11 mM EGTA, 1 mM $CaCl_2$, 1.5 mM Mg-ATP, and 0.3 Li-GTP, pH adjusted to 7.3 with CsOH. The external recording solution consisted of 140 mM NaCl, 5 mM KCl, 2 mM $MgCl_2$, 2 mM $CaCl_2$, 10 mM HEPES, and 11 mM glucose, pH adjusted to 7.4 with NaOH. After the whole-cell configuration was established, an equilibrium period of 10 min was allowed to elapse for establishing adequate solution exchange between the patch pipette and the cell. All recordings were made at a holding potential of −70 mV. Data were filtered at 2 kHz, digitized at 5 kHz, and stored on a laboratory computer using a Digidata 1200 interface and pClamp 8.0 software (Molecular Devices).

Drugs were dissolved in external solution and applied by gravitation, locally to single cells, using a rapid solution exchange system (SF-77B Perfusion Fast-Step, Warner Instruments, Hamden, CT, USA). The 10% to 90% rise time of junction potential at open pipette tip was 1 to 4 ms.

Materials and Drugs. The following pharmacological agents were used: ATP, α,β-methylene ATP lithium salt (α,β-meATP), β,γ-methylene ATP (β,γ-meATP). All drugs were from Sigma (Deisenhofen, Germany) and were prepared as a concentrated stock solution in distilled water and diluted to final concentration in external medium. Throughout this study (except when reproducing experiments with other agonists), we used α,β-meATP as an agonist to avoid interactions between P2Y and $P2X_3$ receptors. HEK293 cells express native G-protein-coupled P2Y receptors, which are activated by the endogenous agonist ATP. It has been shown that G protein activation alters the rates of desensitization and recovery from desensitization of $P2X_3$ receptors (Gerevich et al., 2005, 2007).

Data Analysis. Data were analyzed off-line using pClamp 8.0 software (Molecular Devices). Figures show mean ± S.E.M. values of n experiments. Student's t test was used for statistical analysis. A probability level of 0.05 or less was considered to reflect a statistically significant difference.

Simulations. The simulation was based on a set of differential equations with the occupancy of each receptor state (i.e., the fraction of the receptor population in that specific state) given by the following equation

$$\frac{dS_i(t)}{dt} = \sum_j^n (S_j(t) * k_{ji} - S_i(t) * k_{ij}) \quad (1)$$

where $S_i(t)$ is the occupancy of a specific state at the time t, $S_j(t)$ is the occupancy of a neighboring state (a state in which direct transitions are possible). n is the number of neighboring states, and k_{ij} and k_{ji} are the rate constants of transitions between neighboring states.

All simulations were performed using Berkeley Madonna v8.0.1 (http://www.berkeleymadonna.com/) to solve the differential equations using a fourth-order Runge-Kutta method. All parameters were fitted manually.

Results

Does Equilibrium Distribution of Receptor States Depend on the Initial Distribution? The first question to be answered was whether equilibrium distribution of receptor states indeed depended on their initial distribution as it had been proposed. If this were the case, there would be more than one equilibria, and thus the mechanism would not be compatible with traditional kinetic models; therefore, there would be no point in trying to develop an acceptable one.

To study this question, we investigated the kinetics of recovery from desensitization, and the development of HAD in the presence of nanomolar agonist concentration (10 nM α,β-meATP). After a pulse of 10 μM α,β-meATP, a further 10 nM was superfused for different periods of time (Fig. 1A). Although a single exponential equation does not properly describe the recovery process (e.g., Fig. 6A), the dominant component of recovery could be determined by fitting a single exponential function to the data. The time constant was found to be 309.3 s (Fig. 1B). This time constant should be similar to the time constant of the onset of desensitization in the presence of 10 nM α,β-meATP, because both depend on the same rate constants. We chose to test the 32-min interval, because this is more than five times the apparent time constant. Thus—supposing an exponential time course—the distribution of receptors must be within 1% of the equilibrium distribution. After a 32-min perfusion of 10 nM α,β-meATP, the availability of receptors was tested (using a 10-s pulse of 10 μM α,β-meATP). We found that the presence of preceding agonist pulse did not change the equilibrium; the availability was virtually identical ($p = 0.98$, paired t test, $n = 6$) regardless of the presence or absence of a preceding agonist pulse (Fig. 1C).

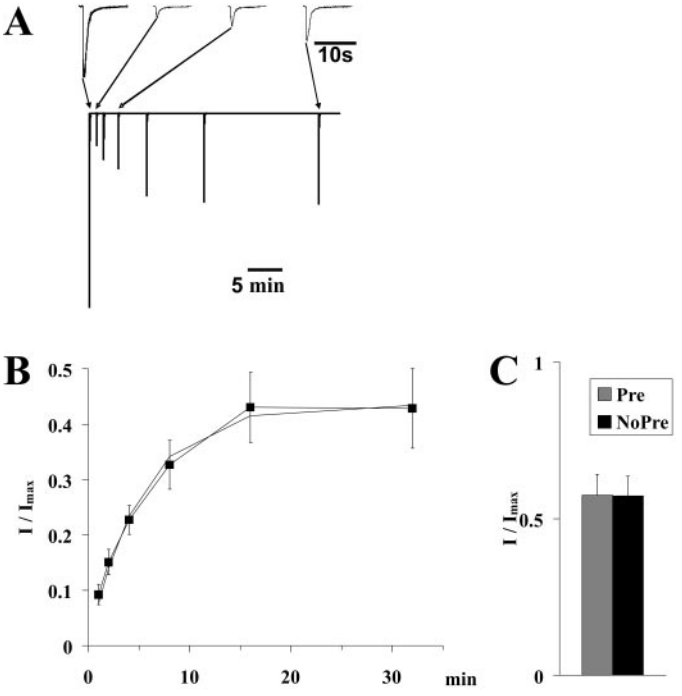

Fig. 1. Equilibrium value of receptor availability in the presence of low agonist concentration. A, superimposed traces show an example of 10 μM α,β-meATP-evoked currents in a cell. First current is an example of control currents (having maximal availability); subsequent currents were evoked after application of 10 nM α,β-meATP for 1, 2, 4, 8, 16, or 32 min. Four of the currents are shown on an expanded time scale (upper panel). Each individual current is normalized to the average of the two control currents evoked before and after it (for this reason, a vertical scale bar is not shown). B, averaged values of recovery from desensitization in the presence of 10 nM α,β-meATP ($n = 5$). Control currents were evoked before each test by a 10s pulse of 10 μM α,β-meATP, then 10 nM α,β-meATP was perfused for one of the following durations: 1, 2, 4, 8, 16, or 32 min, after which the availability of receptors was tested by another 10-s pulse of 10 μM α,β-meATP. Five minutes were allowed for recovery between tests. Data were fitted by a monoexponential function; $\tau = 309.3$ s. C, inhibition by 10 nM α,β-meATP applied for 32 min. No difference in final equilibria was found depending on the initial condition [i.e., between receptors fully desensitized initially by a prepulse of 10 μM α,β-meATP (Pre) and between receptors in initial resting state (NoPre)].

Concentration Dependence of Current Onset and Decay at Low Agonist Concentrations. To construct a model that can reproduce the kinetics of channel behavior throughout an agonist concentration range of several orders of magnitude (from nanomolar to micromolar), it was crucial that reliable records of various concentrations of agonists were available. Measurement of current kinetics can be done most accurately at low agonist concentrations, where activation is slow and therefore not limited by the properties of the drug application system; furthermore, currents are small and therefore not distorted by series resistance error. We used a heterologous expression system to make sure that kinetics of low concentration-evoked currents could be properly measured and were not contaminated by heteromeric $P2X_{2/3}$ receptor-mediated currents (these receptors are also activated by α,β-meATP but have slower kinetics). We measured currents evoked by the following concentrations of α,β-meATP: 100, 178, 316, 562, 1000, 1780, and 3160 nM (Fig. 2). Agonist pulses were given every 5 min. Experiments were started by repeated applications of 316 nM α,β-meATP to ensure the stability of current amplitudes. Once this was established, 316 nM α,β-meATP was applied, alternating with other concentrations, and served as a control throughout the experiment. Each evoked current was normalized to the average of the two neighboring control currents. The amplitude of 316 nM α,β-meATP-evoked currents was fairly stable throughout the experiment; for currents evoked within the first hour of recording, the normalized S.D. was 0.076 $\pm$ 0.031. However, the time constant of current decay increased with recording time monotonically, changing by 54.8 $\pm$ 9.9% ($n = 6$) in an hour. (For all control currents evoked within the first hour, the normalized S.D. was 0.19 $\pm$ 0.07). This change, however, was within the cell-to-cell variance of decay time constants (the normalized S.D. of which was 0.41), and we did not study its origin. Figure 2 illustrates different concentration-evoked currents recorded from a cell. Currents evoked by each concentration were acquired from at least five cells; the averaged traces were used to fit the onset and decay kinetics of simulated currents. The concentration-response curve, based on peak amplitudes, yielded an EC_{50} of 1.29 μM, with an n_H of 1.34.

Construction of the Model. As Sokolova et al. (2006) convincingly argued, the behavior of $P2X_3$ receptors is best described by a circular model in which binding of three agonist molecules is allowed [which is consistent with the trimeric structure of the receptor (Nicke et al., 1998)]. We there-

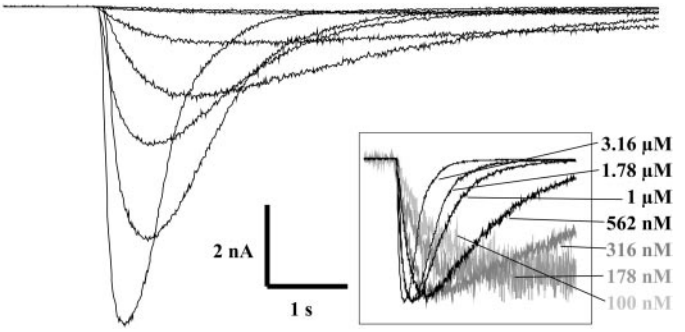

Fig. 2. Currents evoked by the application of α,β-meATP at different concentrations ranging from 100 nM to 3.16 μM. Inset shows normalized current traces to illustrate concentration-dependent changes in onset and decay kinetics.

fore used the scheme of their model as a starting point. Because we have no structural information suggesting that distinct submolecular regions (gates) would be responsible for activation and desensitization, we simplified their scheme and omitted the rapidly developing desensitized state "A_3D_f" (Fig. 3A).

In the case of a circular scheme, the simplest possible way to construct a model is to use the allosteric model of oligomeric proteins as described by Monod et al. (1965). By identifying our model as of "Monod-Wyman-Changeux type" (MWC type) or "allosteric," we mean that it fulfills the following three main conditions: 1) the model is based on the concept that agonists can bind to different conformational states of the receptor but with different affinities; 2) the ratio of affinities is equal to the ratio of gating equilibria with n versus $n + 1$ bound agonists (determined by the "ratio constant" x, as described below); and 3) subunits of the receptor change their conformation in a concerted way. For a more comprehensive description of allosteric models, see Colquhoun (1998) and Karpen and Ruiz (2002).

The first assumption seems to be reasonable and well founded in the case of most receptors. As for the second condition, we consider it a way to reduce the number of free parameters (e.g., from 17 to 8 in the case of our starting model, shown in Fig. 3A), and a way to maintain microscopic reversibility. If MWC-type models constructed using this condition are able to reproduce experimental data well, it will not be a proof that the actual behavior of the receptor agrees with this assumption. The third assumption (i.e., there are no mixed-conformation receptors; e.g., one subunit, open; two subunits, closed) is almost certainly not true for the actual behavior of receptors. Nevertheless, we chose to introduce

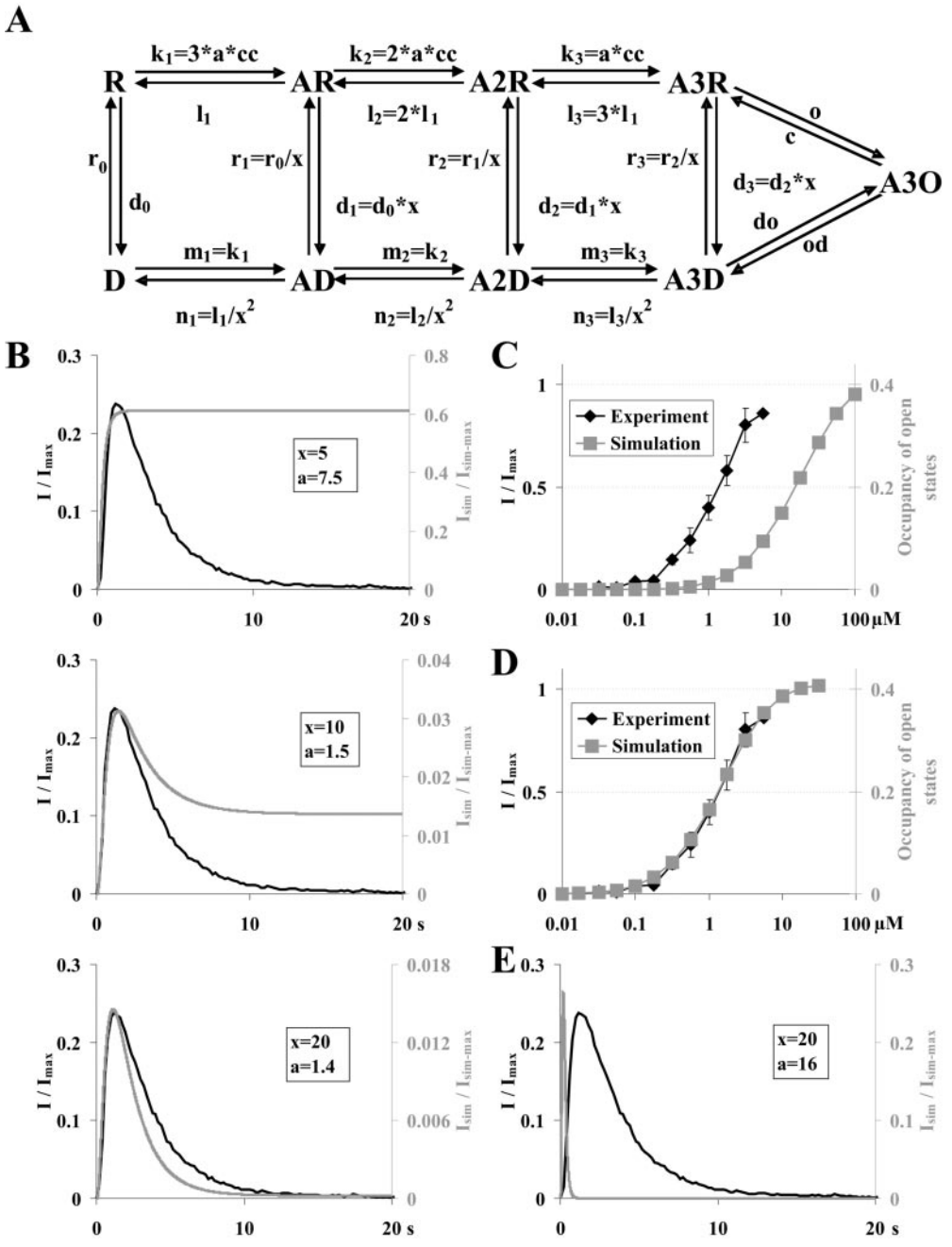

Fig. 3. Simulations using the simplest (one-open-state) model of $P2X_3$ receptors. A, scheme 1 shows the one-open-state model. R, resting states; D, desensitized states; O, open state; A indicates agonist bound states, the number following it indicating the number of bound agonists. Transition rate constants and their calculation are shown next to the arrows. B, simulation of 562 nM α,β-meATP application with different values of the parameter x. The corresponding parameter a was determined for each x by fitting the onset rate of simulated currents to the onset phase of experimentally acquired currents (regardless of the simulated current amplitude). Gray traces, simulated currents; black traces, average ($n = 5$) of experimentally acquired 562 nM α,β-meATP-evoked currents. Values of x and a were 5, 10, and 20 and 7.5, 1.5, and 1.4, respectively. Note the scale of both y axes: the model with parameters x = 20, a = 1.4 seemed to reproduce the currents shape, but with an extremely low amplitude. C, concentration-response curve simulated using the parameters x = 20, a = 1.4. The concentration-response curve is strongly shifted to the right when parameters were determined based on the kinetics and final equilibrium of 562 nM α,β-meATP-evoked currents. ♦, experimentally measured concentration-response curve; gray squares the simulated concentration-response curve. D, when a was determined based on concentration-response data, a = 16 reproduced current amplitudes best. E, simulation of currents using these parameters (x = 20, a = 16) failed to reproduce the kinetics.

this simplification because models without this constraint did not reproduce experimental data significantly better but unnecessarily complicated the scheme of conformations.

For constructing a full allosteric model (Fig. 3A), eight parameters had to be defined (see also Table 1): the concentration-independent term (a) of association rate constants (k_i), the dissociation rate constant (l_1), rate constants of desensitization (d_0) and recovery (r_0) of the vacant receptor, opening (o) and closing (c) rate constants, rate constant of the open-to-desensitized transition (od), and a "ratio constant" (x). The parameters are listed in Table 1.

The ratio constant determined both the ratio of affinities to desensitized versus resting receptors, and the ratio of equilibrium desensitization values with n versus $n + 1$ bound agonist molecules. We found that the model reproduces receptor behavior better if we choose the rate of association to be independent of the conformation (i.e., $k_i = m_i$) and make the rate of dissociation determine preferential affinity to desensitized receptors alone (see Fig. 3A). Using these principles, all other rate constants (k_1, k_2, k_3, l_2, l_3, m_1,m_2, m_3; n_1, n_2, n_3; d_2, d_3, d_4; r_2, r_3, r_4) except reopening from desensitization (do) can be derived, as shown in Fig. 3A, and microscopic reversibility will be maintained. Reopening from desensitization is calculated from rate constants o, c, od, d_4, and r_4.

The opening rate constant (o) was taken from Sokolova et al. (2006). We did not attempt to construct a model that reproduces single channel behavior. Single channel activity was found to be too fast to be resolved, and there was no evidence for a single conductance state (Evans, 1996). Because of these difficulties, no dwell time histograms are yet available, and the origin of fast flickering single channel activity is not known. Therefore, the only limitation for "op" was to be high enough to allow fast activation at high agonist concentrations. Flash photolysis of 100 μM caged ATP resulted in an activation with a 20% to 80% rise time of 20 ms (Grote et al., 2005). This is quite consistent with the rate constant given by Sokolova et al. (2006).

The closing rate constant (c) was chosen to be higher than in the article by Sokolova et al. (2006). Although proper single-channel analysis has not been performed for $P2X_3$ receptors, we can suppose from nonstationary fluctuation analysis data (Grote et al., 2005) that maximal open probability is not higher than ~0.6 to 0.8. Rate constant of desensitization from open state (od) was determined based on the results of Sokolova et al. (2006), where half-times of desensitization converged to ~50 ms at high agonist concentrations.

We introduced a ratio constant (x) that determined both the ratio of affinities to desensitized versus resting receptors and the increase in equilibrium desensitization as a result of the binding of an agonist. For the sake of flexibility, we initially defined three different ratio constants (x, y, and z) to different binding steps. From the simulations (not shown), we later found that having the same constant for all three agonist binding steps was sufficient.

For the determination of the rate constants of desensitization (d) and recovery (r), we had two clues. 1) Rate of recovery was dependent on the agonist; therefore, isomerization of the vacant receptor cannot be rate-limiting (or can only be in the case of the agonist showing the fastest dissociation, which was CTP). Therefore, the rate of desensitization to recovery isomerization (r) must be at least ~0.1 to allow sufficiently rapid recovery from CTP-bound desensitized state (Pratt et al., 2005). 2) We can safely suppose that in the absence of agonists, most receptors are in resting state, therefore d should not be higher than ~0.1.

Dissociation rate constants ("l_i") were determined based on the recovery time constants, supposing that isomerization of vacant receptors is faster; therefore, dissociation from the desensitized receptor (n_1) is rate limiting. From n_1, l_1 can be determined using x (Fig. 3A).

The model constructed this way reproduced experimentally acquired behavior of the receptors rather poorly. To find an optimal set of parameters, we started with optimizing a for current onset rates at different x values. Because at low concentrations association must be the rate-limiting step, the rate of association can be estimated sufficiently well. The best a values for x = 5, 10, and 20 were 7.5, 1.5, and 1.4, respectively (see Table 1). Figure 3B illustrates normalized experimentally obtained currents evoked by 516 nM α,β-meATP and simulated currents. At x = 5 and 10 the current did not desensitize properly (a large plateau current remained). At x = 20, although the kinetics was sufficiently well reproduced, the magnitude of currents was extremely small (the maximal occupancy of open state was ~0.014; note the scale of the right y-axis). The concentration-response curve at x = 20, a = 1.4 was shifted to the right; the EC_{50} was 17 μM (Fig. 3C). When we tried to bring concentration-response curves close to experimental values by increasing a values (Fig. 3D), the onset kinetics became much faster than in experimental data (Fig. 3E).

The problem, as we understood it, was as follows. We know from the decay time constants at high agonist concentration that desensitization from open state is fast ($\tau \approx 50$ ms; see Fig. 1C in Sokolova et al., 2006). If we suppose only one open state (A_3O), then open receptors will isomerize into desensitized conformation with the same rate, irrespective of the overall occupancy of the binding sites in the whole receptor population. For this reason, agonists at low concentration will not evoke significant current, because receptors reach open state at a low rate but desensitize at a constant, high rate. Therefore, to reproduce experimental data, we need slower desensitization from open state at a lower agonist occupancy level. This is only possible if we suppose at least one additional open state with a slower desensitization rate. Thus low agonist concentrations could evoke a relatively large current with slow kinetics, as observed experimentally.

In our next model, therefore, we added an open state of diliganded receptors and initially supposed that diliganded receptors open and close with the same rates as triliganded

TABLE 1
Parameters used in simulations using Scheme 1 (see Fig. 3), Scheme 2 (see Fig. 4), and the two-agonist scheme (see Figs. 5 and 6)

	Scheme 1	Scheme 2	Two Agonist Scheme	
			Drug A	Drug B
a (s^{-1} mM^{-1})	1.4	1.3	1.3	9.75
l_1 (s^{-1} mM^{-1})	0.5	4	4	30
d_0 (s^{-1})	0.002	0.003	0.003	
r_0 (s^{-1})	2.25	0.07	0.07	
o (s^{-1})	65	65		
c (s^{-1})	10	10		
od (s^{-1})	20	20		
x	20	20	20	

ones ($o_2 = o_3$ and $c_2 = c_3$). Because the d_2/r_2 ratio differs from the d_3/r_3 ratio, "od_2" and "do_2" must also differ from "od_3" and "do_3" to preserve microscopic reversibility; they are calculated as: $od_2 = od_3/x$, and $do_2 = do_3 \cdot x$ (Fig. 4A).

As seen in Table 1, value of a only needed a slight adjustment, whereas x remained the same. Rate constants of desensitization and recovery from desensitization of the vacant receptor (d_0 and r_0) were optimized by fitting the concentration-HAD curve (Fig. 4C).

Figure 4B illustrates experimental and simulated agonist-evoked currents at four agonist concentrations: 100, 178, 316, and 562 nM. Concentration-HAD and concentration-peak amplitude curves are shown in Fig. 4C, illustrating data from Pratt et al. (2005), Sokolova et al. (2006), and our current experiments (n = 4 to 8 for each point). (The reason why concentration-HAD curves in the two previous publications differ so much will be discussed below.)

Formation of the High-Affinity Binding Site. A special test revealed a peculiar behavior of $P2X_3$ receptors (Pratt et al., 2005). In a special protocol that we will call the "early-late" protocol, control agonist pulse and test pulse were separated by a long interpulse interval. In either the first or the second half of the interpulse interval, nanomolar agonist was perfused. $P2X_3$ receptors behaved in a remarkably counter-intuitive way: nanomolar agonists caused weak inhibition when applied in the second half of the interpulse interval (i.e., right before the test pulse), but the same concentration of agonist, for the same duration caused a much stronger inhibition when it was applied in the first half (right after the control pulse), even though in this case availability was tested only after a long recovery period.

Nanomolar agonist perfusion during the first half of the interpulse interval was intended to cause inhibition of the test current by stabilizing desensitization, whereas perfusion during the second half was intended to cause inhibition of the test current by inducing desensitization. The fact that the inhibition caused by the early pulse was much more effective indicates that low concentration of the agonist was able to bind to a high-affinity site, which is accessible upon desensitization but becomes inaccessible as recovery from desensitization progresses.

We intended to understand what mechanism can be responsible for this unexpected phenomenon. We started with analyzing a single step within the protocol: the sequence of

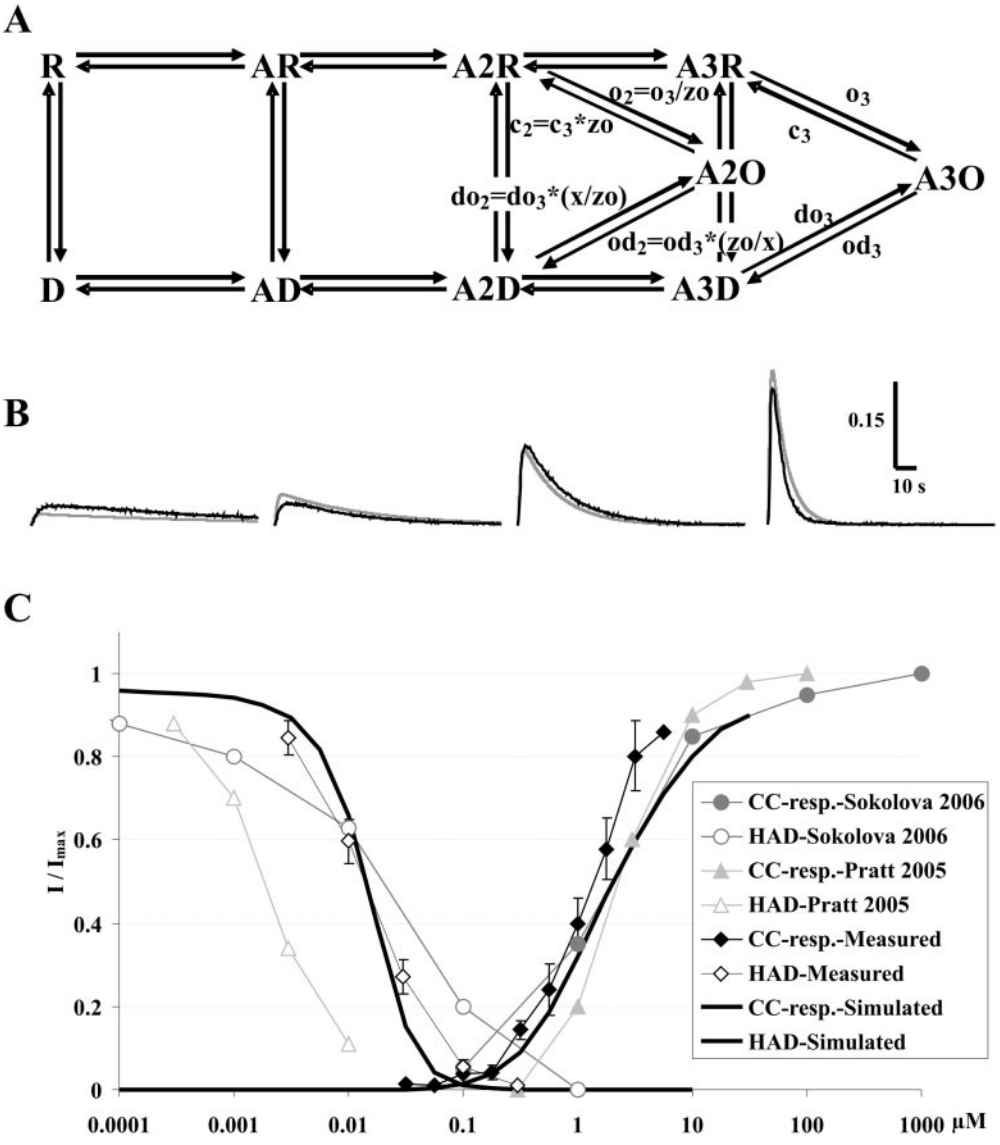

Fig. 4. Simulations using the revised (two-open-state) model of $P2X_3$ receptors. A, scheme 2 shows the two-open-state model. An additional diliganded open state was added. Formulas show the calculation of rate constants for the new transitions. Rate constants for the rest of the transitions are calculated as in the one-open-state-model (see Fig. 3A). B, experimentally acquired (black traces; average of n = 5) and simulated (gray traces) currents evoked by four different concentrations of α,β-meATP (100, 178, 316, and 562 nM). C, concentration-response curves and concentration-HAD curves obtained in three different experimental studies and in simulations. Thick black lines, simulated data; thin lines, experimental data obtained by Pratt et al. (2005) (light gray triangles), Sokolova et al. (2006) (dark gray circles), and the current study (♦). While concentration-response curves are close to each other, concentration-HAD curves differ considerably because of insufficient equilibrium in the experiments of Pratt et al. (2005) (started from fully desensitized receptors; 60 s for equilibration) and Sokolova et al. (2006) (started from resting receptors, 90 s for equilibration). In our current study (◇), we let the receptors equilibrate in the presence of nanomolar concentrations of α,β-meATP for 960 s, which was proven to be enough for equilibration. Simulations were performed using a 2000-s equilibration period for all concentrations.

events taking place during an exchange of agonists. We simulated replacement of a high concentration rapidly dissociating agonist with a low concentration slowly dissociating agonist.

We assumed three binding sites at each receptor, with identical association and dissociation rates for all three sites. No cooperativity of binding was assumed. Because the questions addressed by these simulations are of qualitative nature, the exact values of rate constants are of no importance. The same qualitative results were produced with different types of models and using different parameters, if the following assumptions were made (in accordance with the model of Sokolova et al., 2006). 1) With one of the binding sites occupied, most receptors desensitize. 2) With all three binding sites unoccupied, most receptors recover from desensitized state. 3) The affinity of agonists to desensitized state is much larger than to resting state, which is reflected by a much slower dissociation from desensitized state. 4) Isomerization of vacant receptors from desensitized to resting conformation is relatively fast (i.e., during recovery from desensitization the rate limiting step is dissociation, not isomerization). 5) The rate of agonist association is determined by agonist concentration, and at the studied concentration range (~1 to 100 nM), it is comparable with the dissociation rate. 6) The rate of agonist dissociation is agonist-dependent; for some agonists (e.g., β,γ-meATP) dissociation is faster than for others (e.g., α,β-meATP).

To be able to perform simulations of agonist association and dissociation dynamics with two agonists, we made one additional assumption: 7) Isomerization rates (resting to desensitized and desensitized to resting transition rates) are dependent only on the number of bound agonists and not on which agonist occupies individual binding sites.

Rate constants for the simulations using the scheme shown in Fig. 5A were taken from the model described above (Fig. 4A). Horizontal and vertical transitions show association and dissociation of drug B and drug A, respectively. Desensitized states (subunits marked by circles) are shown in the front, resting states (subunits marked by squares) are in the back. To help comparison, states of Fig. 4A (without open states) are marked by the encircled area. Because this scheme was designed for the study of equilibration at nanomolar agonist concentration, where no significant opening occurs, open states are ignored. Furthermore, because in this specific experiment, when replacement of a rapidly dissociating agonist by a low concentration slowly dissociating agonist is studied, many of the states shown in Fig. 5A do not reach a significant occupancy; these states can be ignored. Figure 5B shows only the states that are relevant in this experiment. (Ignoring the rest of the states does not mean not calculating with them; they are ignored only in the illustration and solely for the sake of clarity.) All shown states reached an occupancy above 0.01 at some time during this simulation experiment, whereas ignored states never exceeded the occupancy value 0.0001 at any time.

For specific parameters used in this simulation, see Table 1. Effects of two fictitious drugs, called drug A (a slowly dissociating agonist) and drug B (a rapidly dissociating agonist) were simulated. In the experiments illustrated here, parameters of drug A were equivalent with parameters of α,β-meATP as used in the simulations shown in Fig. 4. Parameters (association and dissociation rate constants) of the rapidly dissociating agonist, drug B, were chosen so that it roughly reproduced recovery kinetics of β,γ-meATP, but the microscopic affinity was chosen to be the same as in the case of α,β-meATP (i.e., the ratio of a and l_1 was kept constant; see Table 1), so that the effect of difference in association- and dissociation kinetics could be studied separately, not disturbed by a difference in affinity.

Figure 5C illustrates availability of the receptor population as a function of time for three cases: 1) simple association of drug A molecules at a concentration of 10 nM (black line); 2) 10 μM drug B (rapidly dissociating) replaced by 10 nM drug A (slowly dissociating), i.e., dissociation of drug B and association of 10 nM drug A (dark gray line); and 3) 10 μM drug A replaced by 10 nM drug A, i.e., development of the new equilibrium (light gray line). The process we want to analyze is the second case.

During progressive dissociation of drug B and association of drug A, receptors are kept in desensitized conformation provided that at least one of the binding sites is occupied. Desensitized conformation is characterized by a higher agonist affinity, therefore more drug A molecules associate in this state than to resting receptors. Relative occupancy values of states are illustrated at five different times (2, 10, 20, 40, and 1200 s after replacement of 10 μM drug B by 10 nM drug A (Fig. 5D). During dissociation of drug B, association of drug A was already started (Fig. 5D, "2 s"), and although a fraction of receptors loses all its drug B molecules and directly reaches resting vacant state, the majority of receptors will have one or two drug A molecules bound by the time the last drug B molecule dissociates (Fig. 5D, "40 s"). Because one bound agonist is enough to keep the receptor in the high-affinity state, association of drug A molecules will continue to occur despite the low concentration, unless the receptor momentarily loses all three agonists. Whenever this happens, there is a fair chance that isomerization (desensitization state to recovery state transition) occurs sooner than a new association. Once the receptor is isomerized into the low-affinity resting conformation, affinity becomes much less, and most resting receptors remain unoccupied. This way the pool of high-affinity (agonist-bound, desensitized) receptors is slowly drained, and receptors accumulate in the vacant resting state (Fig. 5D, "1200 s"). At equilibrium, a small fraction of resting vacant receptors still binds a single agonist molecule, and among these uniliganded resting receptors, some may desensitize before dissociation. Thus, the final equilibrium will be predominantly determined by the two slowest reactions: association of the first drug A to the vacant low-affinity resting state (this reaction is slow because of the low concentration and the low affinity) and dissociation of the last drug A from the uniliganded high-affinity desensitized state (this reaction is slow because of the high affinity of desensitized receptors). Both isomerization reactions are faster.

The "Early-Late" Protocol Tested in Simulations and Experiments. Having proposed a mechanism of high-affinity binding site formation and the sequence of events during agonist exchange, we analyzed the mechanisms behind the early-late protocol.

We simulated the effects of the two agonists mentioned above: drug B (rapidly dissociating) and drug A (slowly dissociating). First of all, we simulated the rate of recovery from desensitization after drug B and drug A application for com-

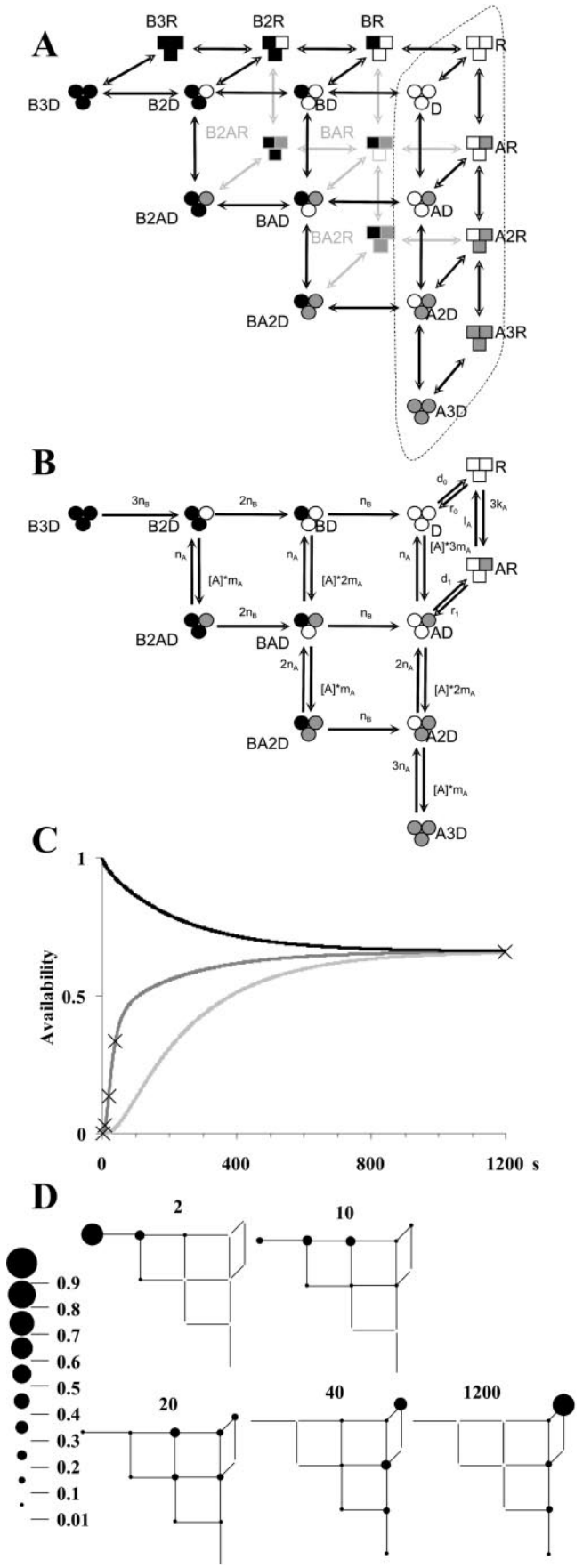

Fig. 5. Simulation of agonist exchange on the receptor binding sites. A, the full model of agonist exchange. Circles and squares represent desensitized and resting receptor conformation, respectively. Open symbols represent subunits with unoccupied binding site; filled symbols represent occupied binding sites (black, drug B; gray, drug A). Horizontal and vertical transitions represent association and dissociation of drug B (rapidly dissociating) and drug A (slowly dissociating), respectively. Diagonal transitions represent isomerization of the receptor. Resting and desensitized states which correspond to those of schemes 1 and 2 are within the encircled area. B, calculation of rate constants shown in the simplified scheme of the model. Association of drug B is not shown, because this was not studied in this particular simulation. States that have not been visited by at least 0.01% of the receptors at any time during the experiment are ignored for better visibility. All shown states have been visited by more than 1% of the receptor population at some time during the experiment. Rate constants: (n_A, n_B, dissociation rate constant for drug A and drug B in desensitized conformation; m_A, association rate constant of drug A in desensitized conformation; l_A, dissociation rate constant for drug A in resting conformation; k_A, association rate for drug A in resting conformation; d_0, d_1, desensitization rate constants at 0 and 1 occupied binding sites, respectively; r_0, r_1, rate constant of recovery from desensitization at 0 and 1 occupied binding sites, respectively; [A], concentration of drug A. C, change of receptor availability in the presence of 10 nM drug A with different initial conditions. Black line, no previous desensitization; light gray line, after full desensitization by the same drug (drug A); dark gray line, after full desensitization by drug B. X marks show times where occupancy of states is illustrated in D. D, the sequence of dissociation and association steps taking place during simulation of replacement of drug B by drug A is illustrated by the relative occupancy values of different states at different time intervals (2, 10, 20, 40, and 1200 s, also shown by X marks in C) after drug exchange. The overall availability during this simulation is illustrated by the dark gray line in C.

parison (Fig. 6A). Then, different interpulse intervals, as well as different combinations of agonists were tested. (By interpulse interval, we mean the time between control and test pulses—illustrated by ▼ in Fig. 6B.) During either the first ("early") or the second ("late") half of the interpulse interval 10 nM agonist A is applied; for illustration, see Fig. 6B.) The effect of different interpulse intervals is shown in Fig. 6B. The dynamics of receptor availability is illustrated by pairs of thin lines for four different interpulse intervals (100, 200, 300, and 400 s; illustrated by the bars below the figure). Lines increasing monotonously in their second section show receptor availability during the early protocol, whereas lines decreasing in their second section show availability during the late protocol. Final availability right before the test pulse (of high concentration agonist) is illustrated by ♦ (early drug application) and ■ (late drug application); simulations were performed with interpulse intervals increasing from 0 to 400 s. It is apparent from the figure that increased potency upon early application is observable only within a definite time window (0–288 s in this case). Because this time window is determined by the ratio of dissociation rates of the two agonists, it is logical to assume that the paradoxical increased potency upon early application will not occur when different concentrations of a single agonist are used. Figure 6C illustrates the plot of final availability as a function of interpulse duration in the case of both drug A (filled symbols) and drug B (open symbols): No matter how long interpulse duration was chosen, early application never caused larger inhibition than late application. This seems logical, because in both early and late protocols, 1) equal time was provided for dissociation of the agonist, so a similar degree of dissociation is expected, and 2) equal time was provided for equilibration in the presence of low concentration agonist, which in the case of early application means dissociation but in the case of late application means association.

As a general conclusion, our simulations suggested that

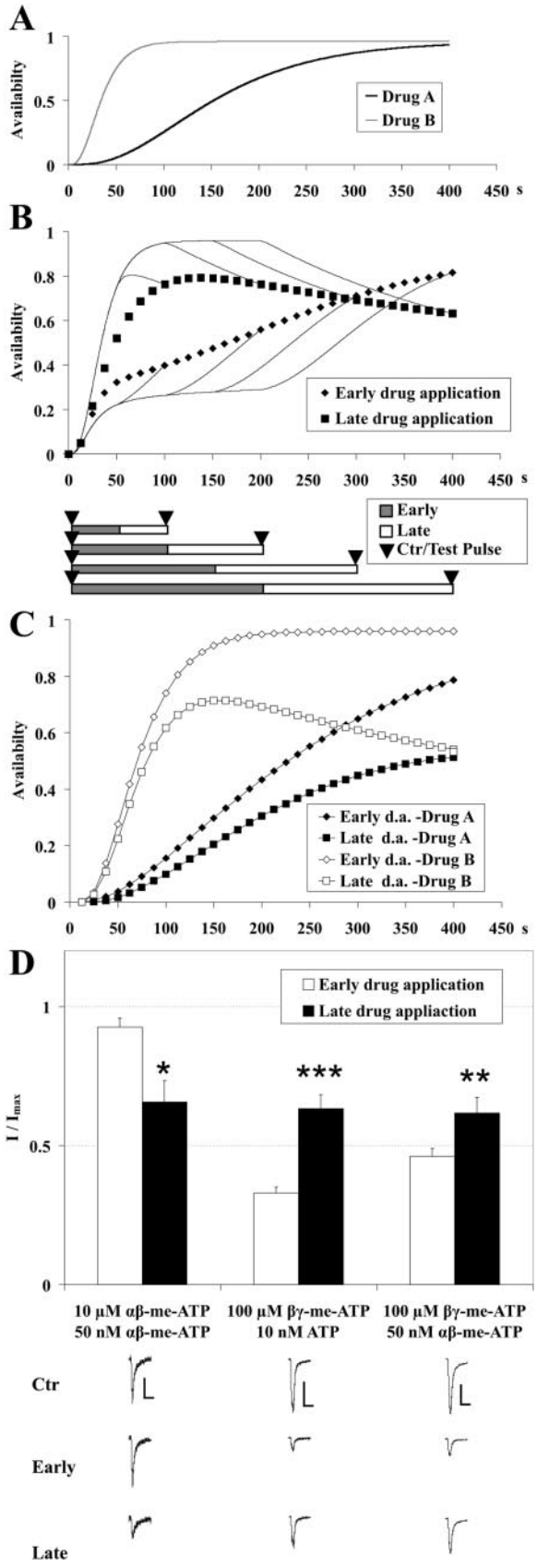

Fig. 6. Simulation of "early-late" protocol using the two-agonist model shown in Fig. 5. A, simulated recovery from inactivation in case of drug B (a rapidly dissociating fictitious drug with dissociation kinetics similar to β,γ-meATP) and drug A (a slowly dissociating fictitious drug, with properties similar to α,β-meATP). After removal of drug B, receptors recover within ~100 s, whereas after drug A, recovery takes ~300 to 400 s. B, simulations show changes in receptor availability during the "early-late" protocol, illustrating that there is a definite time window for the peculiar phenomenon (of early agonist application causing larger inhibition than late agonist application) to develop. High-concentration drug B applications (control and test pulses) are marked by ▼ in the lower panel. At time 0, drug B was removed, and all receptors were in a fully liganded desensitized state from which recovery starts. In the case of "early" protocol, recovery initially proceeds in the presence of 10 nM drug A. It is of moderate rate and converges to the equilibrium availability in the presence of 10 nM drug A. In the case of the "late" protocol, recovery starts in the absence of agonists; therefore, it is rapid and full. Solid lines illustrate availability in the case of four different interpulse intervals (illustrated below the graph). Perfusion of 10 nM drug A was simulated either during the first ("early" protocol) or the second ("late" protocol) half of the interpulse interval. Availability at the end of the interpulse interval is illustrated by diamonds ("early" protocol) or squares ("late" protocol) in 40 different cases (interpulse intervals ranging from 10 to 400 s) C, simulations with different concentrations of a single agonist. The same drug (drug B, open symbols; drug A, closed symbols) was used both at high concentration to evoke initial desensitization and at low concentration to evoke high-affinity desensitization. Availability at the end of the interpulse interval is plotted as the function of interpulse interval duration. Simulations illustrate that "late" application always produces larger inhibition when a single agonist is used. D, inhibition by "early" and "late" application of agonists at low concentrations. Experiments were performed using 10 μM α,β-meATP versus 50 nM α,β-meATP; 100 μM β,γ-meATP versus 10 nM ATP; and 100 μM β,γ-meATP versus 50 nM α,β-meATP. Lower panel shows examples of the currents acquired. Horizontal scalebars, 1 s; vertical scalebars, 0.1 nA (left), 0.4 nA (middle), and 0.6 nA (right). Interpulse interval was determined to match the time required for recovery: 300 s in the case of α,β-meATP and 120 s in the case of β,γ-meATP. As in the simulations, "early" application resulted in larger inhibition only when a slowly dissociating agonist replaced a rapidly dissociating one. Asterisks indicate the level of significance.

the experiment was only able to produce the unexpected increased potency upon early application if two conditions were met: 1) nonequilibrium conditions (i.e., drug application and recovery times had to be short enough compared with the rate of equilibration), and 2) a rapidly dissociating agonist had to be replaced by a slowly dissociating one.

This prediction, that it is impossible to achieve larger inhibition with early agonist application when a single agonist is used, was tested experimentally as well. When we repeated the "early-late" experiment using 100 μM β,γ-meATP and 10 nM ATP, or 100 μM β,γ-meATP and 50 nM α,β-meATP, our results clearly reproduced previous findings of Pratt et al. (2005) and Sokolova et al. (2006). However, when 10 μM α,β-meATP and 50 nM α,β-meATP was used, the late application of the low concentration agonist caused larger inhibition (Fig. 6D).

Discussion

$P2X_3$ receptors desensitize within milliseconds but require several minutes to recover from desensitization. They are activated by micromolar agonist concentrations but effectively desensitized by nanomolar agonist concentrations (Sokolova et al., 2004, 2006; Pratt et al., 2005). Both phenomena originate from the activation and desensitization mechanisms of the receptors, which, however, have not yet been clarified. We aimed to answer some specific questions regarding the mechanism by which $P2X_3$ receptors work and produce the peculiar phenomena described in the cited articles. Answering most questions required not only electrophysiological experiments (in which only conducting and nonconducting states can be separated), but also the additional insight provided by simulations, in which the dynamics of all major conformational states, as well as different degrees of

agonist occupancy, can be monitored, and thus gating mechanism of real receptors can be explored.

The validity of conclusions drawn from simulations obviously depends on whether the model adequately reflects the actual mechanism of receptor activation and desensitization. The fact that the model sufficiently well reproduces all experimental findings (concentration dependence of activation rate, decay rate, current amplitude and HAD as well as recovery rate from desensitization), does not prove this. There are many uncertain points regarding the mechanism of activation and desensitization: Because single channel properties of $P2X_3$ receptors preclude a proper analysis (Evans, 1996), the number of coupled open and closed states, as well as the actual rate constants, cannot be determined. Nevertheless, some conclusions regarding the feasible mechanisms by which $P2X_3$ receptors work can still be drawn.

One conclusion comes from the observation that no matter what type of model we tested, addition of a diliganded open state was necessary to adequately reproduce experimental data. This suggests that a significant fraction of diliganded receptors is likely to reach open conformation. Diliganded open state is characterized by a lower desensitization rate, which means that in the case of prolonged agonist application, low concentration can be as effective as high concentration in terms of cumulative charge flux. A study of mutated heterotrimeric $P2X_{2/3}$ receptors suggests that receptors can open from a less than fully liganded state (Wilkinson et al., 2006). Our findings—obtained by a different approach—suggest that this applies to homomeric $P2X_3$ receptors as well.

Another significant conclusion is that although it seems paradoxical that "early" application of nanomolar agonist is more effective than "late" application, this finding can be conveniently explained by supposing that binding of one agonist molecule increases the affinity of the second and third binding sites. If we assume this, the "paradoxical" behavior emerges whenever 1) the interpulse interval is short enough (i.e., the experiment is done under nonequilibrium conditions) and 2) a rapidly dissociating agonist is exchanged to a slowly dissociating one.

In the light of the results of electrophysiological and simulation experiments we can answer the questions posed in the Introduction:

Does Increased Affinity Indeed Require Preceding Agonist Exposure? Yes and no. Although our model suggests that vacant resting receptors have no high-affinity binding sites, occasional binding nonetheless can happen even at nanomolar agonist concentrations. Whenever binding happens, there is a chance (~5% in our model) that it results in receptor desensitization before dissociation; i.e., high-affinity binding sites are formed. Once desensitized, dissociation is less probable and association is more probable, thus receptors will slowly accumulate in desensitized states, but the final equilibrium will be reached. The rate of equilibration indeed will be considerably higher when previous agonist exposure brings receptors into desensitized (i.e., high-affinity) states, as illustrated in Fig. 5C (black versus dark gray lines), thus in this sense, preceding agonist exposure does enhance high-affinity binding. The affinity of pre-exposed desensitized and non–pre-exposed desensitized receptors, however, will be the same, and so will be the final equilibrium in both experiments. It was observed that a slowly dissociating agonist seems to be far more effective in an experimental protocol in which it is given during pulses of a rapidly dissociating agonist than when given without previous activation (see Fig. 6 in Pratt et al., 2005). This difference does not arise from reaching different equilibria depending on the initial condition but from approaching equilibria at completely different rates. The apparent difference in affinity exists only under nonequilibrium conditions.

Is the High-Affinity Site Different from the Conventional Binding Site? No. In this model the same binding site has different affinities in different conformations (resting or desensitized) of the receptor.

Do We Need to Suppose Unbinding and Rebinding? No. In the model, association of a single agonist molecule is enough to induce desensitization and thus to produce high-affinity binding sites. Having three agonist binding sites per receptor, agonist exchange can take place in a subunit-by-subunit manner, without full dissociation, as shown in Fig. 5D. Unbinding and rebinding, therefore, does occur, but mostly not on the level of receptors, only on the level of receptor subunits. Thus, contrary to what was assumed by Pratt et al. (2005), the desensitized-to-resting isomerization does not need to be slow.

What Is the Mechanism of Binding Site "Transfiguration"? No special mechanism is needed. If we simply assume that agonists have a higher affinity to desensitized receptors, and that binding of one single agonist is able to bring the receptor into desensitized state, high-affinity binding sites will be formed upon association of the first agonist molecule.

Do Low Concentration Agonist-Induced Desensitization and Recovery from Desensitization Converge to the Same Equilibrium Distribution of Receptors? Yes. If enough time is provided for the equilibrium to develop, there will be no difference in the degree of inhibition depending on the starting distribution of receptor conformations, as we have demonstrated by experiments (Fig. 1) and simulations (Fig. 5C). The rate of equilibration is determined by both agonist association and dissociation; therefore, it is lowest at very low concentrations (recovery from desensitization in the presence of 10 nM α,β-meATP proceeded with a time constant of 309 s). Supposing single exponential decay, one must wait roughly $5 \times \tau$ to approach the equilibrium within $\pm$ 1%, which is ~25 min in this case. This is why durations of low concentration agonist application chosen by both Pratt et al. (2005) (60 s for recovery) and Sokolova et al. (2006) (90 s for association) were far too short and thus represent nonequilibrium conditions. This also explains why their HAD versus concentration curves differ so much (Fig. 4C). In our experiments (Fig. 1), we started by assessing the time needed for equilibration and then chose a duration of agonist application which assured that equilibrium is adequately approached.

Can a Conventional Allosteric Model Reproduce Kinetic Behavior of the Receptor? Yes. In fact, we needed a very simple model to accomplish this. There was no need to assign different ratio constants to different binding steps, no need to introduce "cooperativity of binding," and no need to suppose nonconcerted isomerizations of subunits.

The principal question, of course, is not what experiments tell about the properties of the model (i.e., whether we can construct a model that reproduces experimental data), but what the model tells about the object of our experiments (i.e.,

whether our model helps to understand the mechanism behind the properties of the receptor).

Sokolova et al. (2006) argued convincingly that a proper model of the $P2X_3$ receptor must be circular and should have three binding sites. In this article, we add that besides the triliganded open state, a diliganded open state must also be assumed, and that a simple allosteric mechanism can adequately describe the behavior of the receptor, including some phenomena that have gone unexplained, such as the several hundredfold difference between IC_{50} and EC_{50} values, the several thousandfold difference between time constants of desensitization and recovery, and the formation of high-affinity binding sites upon previous agonist exposure. The fact that an MWC-type model so simply explains and so readily reproduces experimentally obtained phenomena, however, certainly does not prove that receptors indeed activate and desensitize by this mechanism (i.e., that subunits of the receptor change their conformation in a concerted manner). Nonconcerted isomerization of subunits has been proven in a number of ion channels (e.g., Chapman et al., 1997; Ruiz and Karpen, 1997; Rosenmund et al., 1998). However, in the case of $P2X_3$ receptors, we must suppose that partial occupancy of agonist binding sites drastically increases the affinity of the rest of (nonoccupied) binding sites; otherwise, no model could reproduce experimental behavior. The MWC model is not the only way but is the simplest way to explain increased affinity of nonoccupied binding sites of partially occupied receptors. One possible alternative mechanism is that although single-subunit isomerizations can happen, neighboring subunits affect each other. Isomerization of a single subunit as a result of agonist binding may increase the probability of isomerization of neighboring subunits, thus affecting the affinity of their binding sites (as it was supposed in the sequential model of Koshland et al., 1966). Further experimental and modeling data will help to refine the molecular mechanisms involved in $P2X_3$ receptor gating.

Acknowledgments

We thank Dr. Rashid Giniatullin for his helpful comments on this manuscript.

References

Chapman ML, VanDongen HM, and VanDongen AM (1997) Activation-dependent subconductance levels in the drk1 K channel suggest a subunit basis for ion permeation and gating. *Biophys J* **72:**708–719.
Colquhoun D (1998) Binding, gating, affinity and efficacy: the interpretation of structure- activity relationships for agonists and of the effects of mutating receptors. *Br J Pharmacol* **125:**924–947.
Evans RJ (1996) Single channel properties of ATP-gated cation channels (P2X receptors) heterologously expressed in Chinese hamster ovary cells. *Neurosci Lett* **212:**212–214.
Fischer W, Wirkner K, Weber M, Eberts C, Koles L, Reinhardt R, Franke H, Allgaier C, Gillen C, and Illes P (2003) Characterization of P2X3, P2Y1 and P2Y4 receptors in cultured HEK293-hP2X3 cells and their inhibition by ethanol and trichloroethanol. *J Neurochem* **85:**779–790.
Gerevich Z, Zadori Z, Müller C, Wirkner K, Schröder W, Rubini P, Illes P (2007) Metabotropic P2Y receptors inhibit $P2X_3$ receptor-channels via G protein-dependent facilitation of their desensitization. *Br J Pharmacol* **151:**226–236.
Gerevich Z, Müller C, Illes P (2005) Metabotropic P2Y1 receptors inhibit P2X3 receptor-channels in rat dorsal root ganglion neurons. *Eur J Pharmacol* **521:** 34–38.
Grote A, Boldogkoi Z, Zimmer A, Steinhauser C, and Jabs R (2005) Functional characterization of P2X3 receptors fused with fluorescent proteins. *Mol Membr Biol* **22:**497–506.
Karpen JW and Ruiz M (2002) Ion channels: does each subunit do something on its own? *Trends Biochem Sci* **27:**402–409.
Koshland DE Jr, Nemethy G, and Filmer D (1966) Comparison of experimental binding data and theoretical models in proteins containing subunits. *Biochemistry* **5:**365–385.
Monod J, Wyman J, and Changeux JP (1965) On the nature of allosteric transitions: a plausible model. *J Mol Biol* **12:**88–118.
Nicke A, Baumert HG, Rettinger J, Eichele A, Lambrecht G, Mutschler E, and Schmalzing G (1998) P2X1 and P2X3 receptors form stable trimers: a novel structural motif of ligand-gated ion channels. *EMBO J* **17:**3016–3028.
North RA (2002) Molecular physiology of P2X receptors. *Physiol Rev* **82:**1013–1067.
Pratt EB, Brink TS, Bergson P, Voigt MM, and Cook SP (2005) Use-dependent inhibition of P2X3 receptors by nanomolar agonist. *J Neurosci* **25:**7359–7365.
Rettinger J and Schmalzing G (2003) Activation and desensitization of the recombinant P2X1 receptor at nanomolar ATP concentrations. *J Gen Physiol* **121:**451–461.
Rosenmund C, Stern-Bach Y, and Stevens CF (1998) The tetrameric structure of a glutamate receptor channel. *Science* **280:**1596–1599.
Ruiz ML and Karpen JW (1997) Single cyclic nucleotide-gated channels locked in different ligand-bound states. *Nature* **389:**389–392.
Sokolova E, Skorinkin A, Fabbretti E, Masten L, Nistri A, and Giniatullin R (2004) Agonist-dependence of recovery from desensitization of P2X(3) receptors provides a novel and sensitive approach for their rapid up or downregulation. *Br J Pharmacol* **141:**1048–1058.
Sokolova E, Skorinkin A, Moiseev I, Agrachev A, Nistri A, and Giniatullin R (2006) Experimental and modeling studies of desensitization of $P2X_3$ receptors. *Mol Pharmacol* **70:**373–382.
Wilkinson WJ, Jiang LH, Surprenant A, and North RA (2006) Role of ectodomain lysines in the subunits of the heteromeric $P2X_{2/3}$ receptor. *Mol Pharmacol* **70**: 1159–1163.

Address correspondence to: A. Mike, Institute of Experimental Medicine, Hungarian Academy of Sciences, P.O. Box 67, H-1450 Budapest, Hungary. E-mail: mike@koki.hu